α-D-Glucan-Based Dendritic Nanoparticles Prepared by in Vitro Enzymatic Chain Extension of Glycogen

Jean-Luc Putaux,[†] Gabrielle Potocki-Véronèse,[‡] Magali Remaud-Simeon,[‡] and Alain Buleon*,[§]

Centre de Recherches sur les Macromolécules Végétales, ICMG-CNRS, BP 53, F-38041 Grenoble Cedex 9, France (affiliated with the Joseph Fourier University of Grenoble), Laboratoire Biotechnologie-Bioprocédés, UMR INRA 792, UMR CNRS 5504, INSA DGBA, 135 avenue de Rangueil, F-31077 Toulouse Cedex 4, France, and INRA, Rue de la Géraudière, BP 71627, F-44316 Nantes Cedex 3, France

Received December 22, 2005; Revised Manuscript Received March 17, 2006

The recombinant amylosucrase from *Neisseria polysaccharea* was used to glucosylate glycogen particles in vitro in the presence of sucrose as the glucosyl donor. The morphology and structure of the resulting insoluble products were shown to strongly depend on the initial sucrose/glycogen weight ratio. For the lower ratio (1.14), all glucose molecules produced from sucrose were transferred onto glycogen, yielding a slight elongation of the external chains and their organization into small crystallites at the surface of the glycogen particles. With a high initial sucrose/glycogen ratio (342), the external glycogen chains were extended by amylosucrase, yielding dendritic nanoparticles with a diameter 4−5 times that of the initial particle. A partial crystallization of the elongated chains induced a "shrinkage" of the nanospheres. The synthesis of linear α-(1,4) chains occurred simultaneously, yielding semicrystalline fibrous entities. All products displayed a B-type crystal structure. The kinetics of chain elongation and aggregation were thoroughly investigated in order to explain how the action of amylosucrase resulted in such different structures. These results emphasize the potentiality of amylosucrase in the design of original carbohydrate-based dendritic nanoparticles.

Introduction

Glycogen is a storage form of glucose occurring mainly throughout the animal kingdom,[1−4] in mammalian cells and shellfish. Glycogen-like molecules, known as phytoglycogen, have also been reported to accumulate in the place of or in addition to starch in mutants of plants such as maize,[5] sorghum,[6] rice,[7] or algae.[8] In maize, phytoglycogen is a major component of the sugary 1 (*su*1) mutant[9] which was shown to lack a specific form of debranching enzyme with isoamylase-like specificity.[10] Glycogen consists of linear chains of α-(1,4)-linked glucose residues, which are interlinked by α-(1,6) glucosidic bonds, yielding a molecular weight of about 10^7. The fine structure and branched nature of glycogen have been widely studied using a combination of high-performance size exclusion chromatography and repeated enzymatic treatments with α-amylase and pullulanase.[2−4,11−13] In average the individual linear chains are composed of between 10 and 14 glucose residues. There is approximately 1 branching point for 10 glucose residues, which is twice the value usually found for amylopectin. The resulting structure is highly branched. The structure of phytoglycogen is very similar to that of glycogen with almost identical chain lengths.[5,9,14]

Several structural models in agreement with these data have been proposed to describe glycogen molecules (see reviews in refs 1−4). A fractal structure was proposed by Melendez et al.[15] in relation to the biosynthetic pathway of glycogen and the way it is degraded by phosphorylase. A model of random dendritic architecture, without spatial restriction induced by interaction between external chains, was also built by Caldwell and Matheson[16] using the characteristic chain distribution and branching pattern known in glycogen.

Several authors have studied the morphology of glycogen using transmission electron microscopy (TEM) images of negatively stained preparations.[12,17−20] It has been described in terms of rosette-like α-particles, which were shown to be aggregates of smaller spherical β-particles, with a mean diameter of 20−30 nm. In recent years, cryo-TEM, which allows observation of objects embedded in a thin film of vitreous ice, has proven to be a useful method to analyze the morphology and size distribution of individual or aggregated nanoparticles in suspension, without artifactual drying and/or staining effects.[21] It has been used by Putaux et al.[22] to study the morphology of phytoglycogen. The particle size drawn from quasi-elastic light scattering data was compared with that measured from images recorded using cryo-TEM and TEM coupled with negative staining or tungsten−tantalum shadowing.

The in vitro enzymatic modification of glycogen through chain elongation has also been attempted using amylosucrase from *Neisseria polysaccharea*. This enzyme has been extensively studied, especially as a recombinant enzyme, as its catalytic properties present an applicative interest for the in vitro synthesis and modification of starchy products. From sucrose as the sole substrate, it catalyzes the synthesis of a linear α-(1,4)-glucan (amylose-like polymer) and releases fructose.[23] The reaction starts by sucrose hydrolysis. The glucose formed is then used as acceptor of the glucosyl units coming from sucrose to produce, after successive transfers via a multichain elongation process, maltooligosaccharides and longer α-(1,4) chains which

* Corresponding author. E-mail: buleon@nantes.inra.fr. Fax: 33 240 67 50 43.
[†] Centre de Recherches sur les Macromolécules Végétales.
[‡] Laboratoire Biotechnologie-Bioprocédés.
[§] INRA.

10.1021/bm050988v CCC: $33.50
Published on Web 05/03/2006

precipitate when they reach a critical size and concentration.[24] The resulting particles exhibit an exceptionally high B-type crystallinity, an original axialitic or spherulitic structure,[25] and a high resistance to digestive enzymes. The glucosylation of the fructose released in the medium also occurs as a side reaction to form sucrose isomers.[23−25] Moreover, this enzyme is able to glucosylate various exogenous acceptors, like α-(1,4)/α-(1,6)-glucans,[26] to the detriment of sucrose hydrolysis and oligosaccharide synthesis, depending on the sucrose/acceptor ratio.[27] Amylosucrase catalyzes the elongation of some external chains of the acceptor molecule, increasing their molecular weight and gyration radius.[26−28] The resulting polysaccharides display interesting gel properties and resistant starch content,[26] dependent on the acceptor structure. Among the tested acceptors, glycogen is particularly efficiently glucosylated by amylosucrase. Indeed, the reaction rate is 100-fold increased by the addition of 30 g/L glycogen to 100 mM sucrose.[27] Amylosucrase 3-D structure analyses revealed the presence of surface oligosaccharide binding sites, suggested to be involved in the positioning of glycogen external chains. This enabled us to propose a molecular model describing the elongation through a semiprocessive mode where the oligosaccharide binding sites would play the role of chain anchoring.[29]

This work investigates the modifications undergone by glycogen particles during their glucosylation by amylosucrase. On the basis of biochemical analyses, conventional TEM and cryo-TEM observation, as well as X-ray diffraction (XRD) data, it provides new insights into the control of the chain elongation kinetics as well as the resulting morphology and crystallinity of the synthesized products. The potential use of the nanoparticles as matrixes with specific properties (ligand complexation, resistance to α-amylases) or as a biomimetic system used to understand the biosynthesis of starch granules is also briefly discussed.

Experimental Section

Enzyme Extraction and Purification. Recombinant *E. coli* strain BL21 carrying the pGST-AS plasmid was used to produce the fusion protein glutathione-S-transferase/amylosucrase (GST-AS), which was further purified by affinity chromatography using glutathione-sepharose 4-B (Amersham-Pharmacia), as previously described.[28] As the GST-AS fusion protein displays the same catalytic properties as the purified amylosucrase (data no shown), the glutathione-S-transferase tag was not removed to catalyze glycogen glucosylation.

In Vitro Glucosylation of Glycogen by Amylosucrase. The synthesis reactions were performed at 30 °C in 50 mM Tris−HCl buffer, pH 7.0, supplemented with 100 mM (34.2 g/L) sucrose and 0.5 U/mL of GST-AS. One unit of amylosucrase corresponds to the amount of enzyme that catalyzes the production of 1 μmol of fructose per min in the presence of 50 g/L sucrose and 0.1 g/L glycogen. Two concentrations of oyster glycogen (provided by INRA, Nantes, France), namely, 0.1 g/L and 30 g/L, corresponding to high (342 w/w) and low (1.14 w/w) sucrose/glycogen ratios, respectively, and referred to as HSGR and LSGR conditions in the following, were tested in order to determine the impact of the acceptor concentration on the chain elongation and organization of the synthesized product. At different reaction times, samples of the reaction medium were collected and submitted to the action of 23 μg/mL proteinase K during 5 min at 37 °C to degrade GST-AS and stop the reaction.

Carbohydrate Analysis. The soluble fraction and precipitate formed during the reaction were separated by centrifugation (10 min, 10 000 g). The soluble fraction was analyzed by high-performance anion exchange chromatography with pulsed amperometric detection (HPAEC−PAD) on a 4 × 250 mm Dionex Carbopac PA100 column to quantify sucrose, glucose, fructose, turanose, and trehalulose. A gradient of sodium acetate (from 6 to 300 mM in 28 min) in 150 mM NaOH was applied at a 1 mL/min flow rate. Detection was performed using a Dionex ED40 module with a gold working electrode and a Ag/AgCl pH reference.

The products resulting from the debranching of modified glycogen were analyzed by HPAEC−PAD, and the length distribution of the α-(1,4) chains was determined. The debranching medium was directly injected in the HPAEC−PAD system, and a gradient of sodium acetate was applied as follows: 0−2 min, 0 mM; 2−12 min, 0−225 mM; 12−47 min, 225−300 mM; 47−111 min, 300−450 mM.

The amount of glucosyl units incorporated into the various α-glucans was determined from high-performance size exclusion chromatography (HPSEC) analyses. For each sample, 100 μL of the entire reaction medium (containing soluble and precipitated products) was solubilized by addition of 25 μL of 5 N NaOH during 1 min at 80 °C. Samples were then diluted by the addition of 187.5 μL water and neutralized by addition of 312.5 μL 0.4 N HCl. The samples corresponding to reactions carried out using 30 g/L glycogen were twice diluted before solubilization. In all cases, the resulting samples contained 200 mM NaCl. They were immediately injected into the HPSEC system to avoid any reprecipitation of the α-glucans. HPSEC analyses were performed on a series of columns (Shodex OH−PAK SB-804 and KB-803), using a Hewlett-Packard 1050 series chromatographic system consisting of a pump, an automatic injector, and an HP 1047A refractometer. Sugars were eluted at 50 °C with 200 mM sodium chloride at 0.55 mL/min.

The HPSEC system was calibrated using glucose, maltoheptaose, initial glycogen, and amylose produced by amylosucrase using 600 mM sucrose.[25] Sugar sample recovery calculated from the area of the refractive index profiles of the samples collected at different reaction times was always higher than 99%.

The amount of linear α-(1,4) chains (DP ≥ 2) was calculated as the difference between the total amount of sugars of size inferior to that of initial glycogen (corresponding to retention times higher than the maximum retention time of the peak of the initial glycogen) and the amounts of sucrose, glucose, fructose, turanose, and trehalulose determined by HPAEC. For the reaction catalyzed from 0.1 g/L glycogen and 100 mM sucrose, the glycogen and modified glycogen were not sufficiently concentrated in the analyzed samples to quantify them directly from their area. Consequently, the concentration of modified glycogen was calculated as follows:

$$\begin{aligned}[\text{modified glycogen}] = {} & [\text{initial glycogen}] + \\ & [\text{consumed sucrose}] - [\text{linear } \alpha\text{-(1,4)-chains}] - \\ & [\text{trehalulose}] - [\text{turanose}] - [\text{glucose}] - [\text{fructose}]\end{aligned}$$

For the samples corresponding to reactions carried out using 30 g/L glycogen and 100 mM sucrose, the amount of modified glycogen was directly measured using the area of the corresponding peak on HPSEC profiles.

Complexation of α-(1,4) Chains with Iodine. The iodine-binding properties of the α-(1,4) chains contained in the reaction media (elongated chains of the modified glycogen and linear glucans synthesized from sucrose by amylosucrase) were studied. The average chain length was determined using the maximum absorption wavelength (λ_{max}) of the α-(1,4) chains/iodine complexes. At various reaction times, the products contained in the reaction medium were diluted 100 times in water and solubilized by heating at 130 °C in an oil bath during 30 min. A 200-μL sample of the solubilized reaction medium was mixed with 20 μL of aqueous iodine solution (2% w/v KI, 0.2% w/v I_2) and 5 μL of 0.1 M HCl in microtiter plates. The λ_{max} of the α-(1,4) chains/iodine complexes was determined by recording spectra between 450 and 700 nm with 2 nm steps, using a Sunrise spectrophotometer (Tecan, Switzerland). The corresponding $\overline{DP}$ was calculated using the equation previously established for amylose chains with $\overline{DP}$ ranging from 28 to 70:[30]

$$10^3/\lambda_{max} = 11.6/\overline{DP} + 1.537$$

Debranching Experiments. Debranching experiments were performed using isoamylase from Hayashibara (Japan). The products contained in the reaction medium were diluted 100 times in water, solubilized by heating at 130 °C in an oil bath during 30 min, and progressively cooled to 50 °C in a water bath. For 10 mL of diluted reaction media, 113 μL of 0.001 N HCl was added to decrease the pH from 7.0 to 4.0. Immediately after, 0.22 μg (13 units) and 4.8 μg (283 units) of isoamylase was added to the reaction media obtained in HSGR and LSGR conditions, respectively. Debranching was performed during 60 h at 50 °C. To determine the length of the external chains in initial glycogen, debranching was performed in LSGR conditions on a sample containing 34.2 g/L sucrose, 30 g/L initial glycogen, and 50 mM Tris, pH 7.0.

Transmission Electron Microscopy. At definite incubation times, after having stopped the enzymatic reaction by adding proteinase K, the entire samples were diluted in distilled water prewarmed at 37 °C and used to prepare specimens for TEM observation. Droplets of the suspensions were deposited onto glow-discharged carbon-coated microscopy grids. After 1 min, the liquid in excess was blotted, and prior to drying, a drop of 2% (w/v) uranyl acetate negative stain was added. After blotting the stain in excess, the residual liquid film was allowed to dry. For the reactions carried out using 0.1 g/L glycogen, the sample obtained after an incubation of 2 h 45 min was difficult to observe, probably due to the high concentration of unconsumed sucrose. Consequently, an additional washing step was carried out just after deposition of the sample and blotting of the excess liquid. A drop of distilled water was deposited onto the grid, the liquid in excess blotted, and the negative stain added.

Specimens for cryo-TEM were prepared as described elsewhere.[21,22] Thin films of suspensions were formed on "lacey" carbon membranes (NetMesh, Pelco, U.S.A.) and vitrified in liquefied ethane using a Leica EMCPC fast-freezing station. The grids were mounted in a Gatan 626 cryo-holder precooled with liquid nitrogen, transferred in the microscope, and observed at low temperature (−175 °C), under low-dose illumination. All samples were observed using a Philips CM200 "Cryo" microscope operating at 80 kV. Images were recorded on Kodak SO163 films, at a magnification of 27 500×. The low-dose procedure developed by Philips was used for cryo-TEM specimens in order to limit radiation damage in the areas of interest prior to image recording. Selected negatives were digitized with a Kodak Megaplus CCD camera, and particle size measurement was performed using the ImageJ software (http://rsb.info.nih.gov/ij/).

X-ray Diffraction. After having removed the soluble fraction of the samples by centrifugation (10 min, 10 000 g), the precipitates were washed three times using one volume of distilled water and finally one time using one volume of water containing 0.02% NaN_3. XRD was performed after adjustment of the water content of the washed precipitates by water desorption at 90% relative humidity (RH), for 10 days under partial vacuum in the presence of a saturated barium chloride solution. The samples (20 mg) were then sealed between two tape foils to prevent any significant change in water content during the measurement. Diffraction diagrams were recorded using an INEL (Artenay, France) spectrometer operating at 40 kV and 30 mA in the Debye−Scherrer transmission mode. The X-ray radiation Cu Kα_1 ($\lambda = 0.15405$ nm) was selected with a quartz monochromator. Diffraction diagrams were recorded during 2 h exposure periods, with a curve position sensitive detector (INEL CPS 120). Relative crystallinity was determined after normalization of all recorded diagrams at the same integrated scattering between $2\theta = 3°$ and 30°. Spherulitic B-type recrystallized amylose was used as a standard, after scaled subtraction of an experimental amorphous curve in order to get null intensity in the regions without diffraction peaks. Dry extruded potato starch was used as the amorphous standard.

The degree of crystallinity was determined using the method initially developed by Wakelin et al. for cellulose.[31] The lateral crystal size along the *a*-axis of the unit cell was approximated from the half-peak width of the 100 reflection ($2\theta \approx 5.6°$) using the Scherrer equation: $d_{hkl} = K\lambda/B \cos\theta$ where B is the half-peak width, λ the radiation wavelength, d_{hkl} the average length of the diffracting domains normal to the family of planes (*hkl*), and K a constant usually taken as 0.9 for starch and cellulose.[32]

Table 1. Amounts of the Various Products Synthesized from 34.2 g/L Sucrose, in the Presence of 0.1 and 30 g/L Glycogen[a]

glycogen content (g/L)	reaction time	sugar and α-glucan concentration (g/L)			
		glucose	sucrose isomers	linear α-(1,4) chains	modified glycogen
0.1	1 h	0.3	0.6	3.2	0.4
	2 h 45 min	0.6	2.2	3.2	0.8
	7 h 20 min	0.6	4.2	5.3	2.2
	13 h	0.7	5.8	9.9	2.2
	23 h	0.8	6.8	10.0	2.2
30	1 h	0.1	0.3	0	46.8

[a] Sucrose consumption values were 95% and 100% after 23 h using 0.1 g/L glycogen and 1 h using 30 g/L glycogen, respectively.

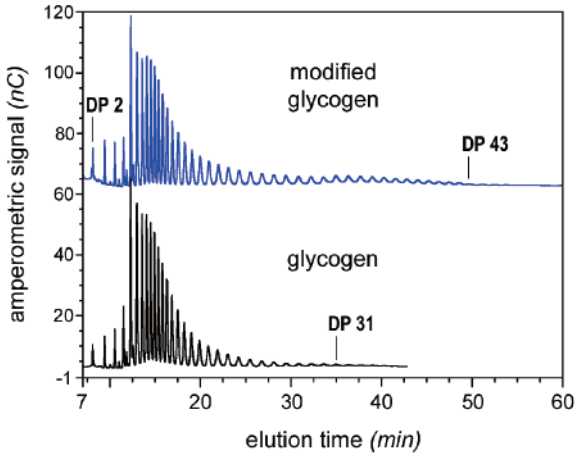

Figure 1. HPAEC-PAD profiles of the linear α-(1,4)-glucan chains obtained by debranching with isoamlyase initial glycogen particles and the product prepared during a 4 h incubation in low sucrose/glycogen ratio conditions.

Results

Kinetics and Yield of α-Glucan Polymerization, Product Chain Length. The sucrose quantification by HPAEC confirmed that the reaction carried out using LSGR conditions was the fastest, as initial sucrose was totally consumed in 1 h, while the substrate consumption was 95% complete only after 23 h using HSGR conditions. Moreover, the amounts of the various synthesized products clearly depended on the initial sucrose/glycogen ratio (Table 1). With LSGR conditions, 99% of the glucosyl units coming from sucrose were incorporated into glycogen, the rest being used to coproduce sucrose isomers and glucose. No trace of any other product was visible on HPAEC or HPSEC profiles at any reaction time. The λ_{max} value of the modified glycogen complexed with iodine was 534 nm (which corresponds to $\overline{DP}$ 34), while initial glycogen did not complex iodine. The HPAEC-PAD profile of glycogen debranched using isoamylase (Figure 1) revealed the presence of linear α-(1,4) chains with DP 2−31, the largest population being that of DP 6−15 chains. The DP of the linear chains of the debranched glucosylated glycogen reached 43.

On the contrary, amylosucrase was very polyspecific when the reaction was carried out using HSGR conditions. The amount

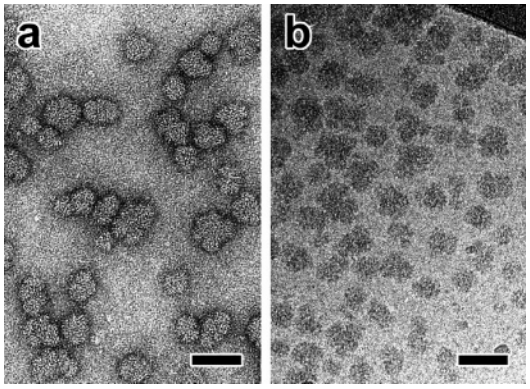

Figure 2. TEM images of initial oyster glycogen particles: (a) after negative staining; (b) embedded in a thin film of vitreous ice. Scale bars: 50 nm.

Table 2. Mean Diameters, in Number D_n (standard deviation in brackets) and in Weight D_w, as Well as Polydispersity Index (P) Measured from TEM Images of 700 Oyster Glycogen Particles in Negatively Stained and Ice-Embedded Specimens

TEM specimen preparation	D_n (nm) [standard deviation]	D_w (nm)	P
negative staining	29.4 [7.0]	34.7	1.18
cryo-TEM	26.1 [6.0]	30.7	1.17

of glucosyl units incorporated into the modified glycogen only reached 21% of the glucosyl units coming from the consumed sucrose at 7 h 20 min reaction. The amount of modified glycogen (2.2 g/L, which corresponds to 12% of the total incorporable glucosyl units coming from the initial sucrose) did not increase afterward. The amount of glucosyl units incorporated into linear α-(1,4) chains reached 54% and 61% of the glucosyl units coming from the consumed sucrose at 7 h 20 min and 23 h, respectively. The corresponding concentrations of linear α-(1,4) chains are 5.3 g/L (31% of the total incorporable glucosyl units coming from the initial sucrose) and 10 g/L (58% of the total incorporable glucosyl units coming from the initial sucrose) at 7 h 20 min and 23 h, respectively. The yield of linear α-(1,4) chain synthesis strongly increased after 7 h 20 min when glycogen elongation stopped. At the final time, the amount of sucrose isomers was also much higher than for the reaction carried out using 30 g/L glycogen.

The λ_{max} value of the HSGR reaction products complexed with iodine was 596 nm at 2 h 45 min, 614 nm at 7 h 20 min, and 610 nm at 23 h, which corresponds to $\overline{DP}$ 82, 127, and 113, respectively. HPSEC profiles (data not shown) of the HSGR reaction products, obtained for reaction times above or equal to 7 h 20 min, revealed the presence of a polymer whose length corresponded approximately to that of the amylose-like chains produced from 600 mM sucrose alone ($\overline{DP}$ 35).[25] Solubilization of the products in water at 130 °C, in 5 or 20 times diluted reaction media revealed impossible. A 100 times dilution was necessary to achieve solubilization and therefore allow subsequent debranching. However, in these conditions, the resulting debranched products were not sufficiently concentrated to be detected either by HPAEC-PAD or by HPSEC.

Morphology of the Initial Glycogen. TEM images of initial oyster glycogen particles are shown in Figure 2. The diameter of 700 particles was measured from the electron micrographs of negatively stained (Figure 2a) and ice-embedded (Figure 2b) preparations (Table 2). Number and volume average diameters as well as polydispersity indexes ($\overline{D_n}$, $\overline{D_w}$, and P, respectively) were calculated using the expressions given by Putaux et al.[22]

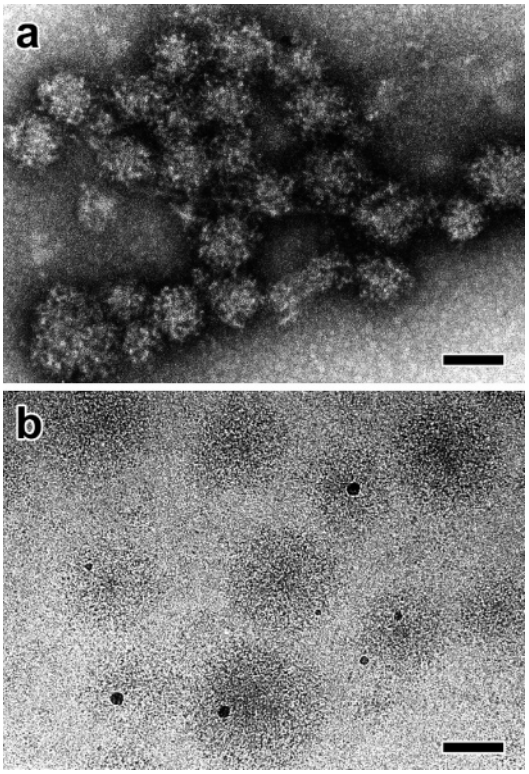

Figure 3. TEM images of the product obtained after a 2 h 45 min incubation in high sucrose/glycogen ratio conditions: (a) negative staining; (b) cryo-TEM. The small dark particles correspond to contamination ice crystals.

The dried and stained particles appear to be slightly larger than those embedded in vitreous ice ($\overline{D_w}$ = 34.7 nm and $\overline{D_w}$ = 30.7 nm, respectively). The diameter is smaller than that measured in similar conditions from phytoglycogen particles extracted from the *su*1 maize mutant ($\overline{D_w}$ = 53.8 nm and $\overline{D_w}$ = 65.7 nm, respectively).[22]

The size measurements performed on TEM images can be compared to the data obtained by HPSEC coupled with multiangle laser light scattering (MALLS). A gyration radius of 20.0 nm was reported for oyster glycogen by Potocki de Montalk et al.,[28] corresponding to a diameter of 40.0 nm. Light scattering data thus provides a size that is about 10 nm larger than that determined from cryo-TEM images. The difference is on the same order as that reported by Putaux et al. for phytoglycogen.[22] A similar effect was recently discussed by Durrieu et al. regarding measurements performed on various suspensions of polyurethane nanoparticles.[34] For both techniques, the detection is based on different properties of the particles. In particular, light scattering gives more statistical "weight" to the larger particles which scatter more strongly.

Morphology of the Product Obtained after Enzymatic Action. *High Sucrose/Glycogen Ratio.* TEM images of the product obtained with HSGR conditions after an incubation of 2 h 45 min are shown in Figure 3. Differences can be seen depending on the way the samples were prepared. After negative staining and drying, aggregates of spheroidal particles with an irregular surface are observed, their apparent diameters ranging from 80 to 180 nm, with an average value of about 100 nm (Figure 3a). Images from the fast-frozen suspension show rather well individualized spheroidal particles with an average diameter of 150 nm (range 100−200 nm) (Figure 3b). Most particles exhibit a slightly darker core, the effect being more clearly seen on the larger objects. Considering the imaging conditions (1−2

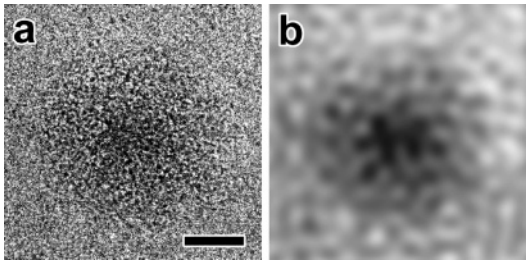

Figure 4. (a) Cryo-TEM image of a spherical particle observed after a 2 h 45 min incubation in high sucrose/glycogen ratio conditions (scale bar: 50 nm); (b) corresponding low-pass Fourier-filtered image enhancing the core−shell aspect of the particle.

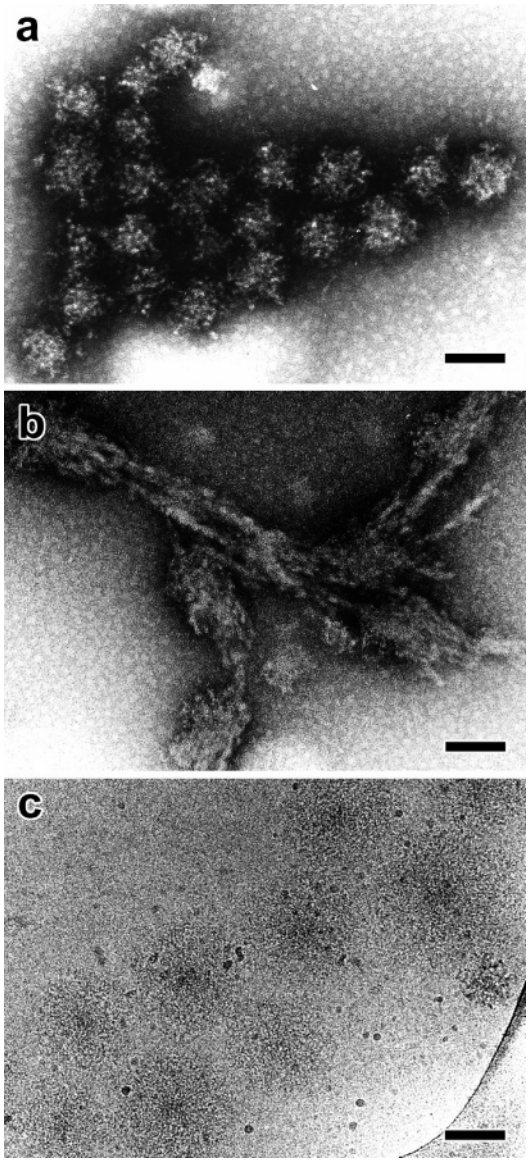

Figure 5. TEM images of the product obtained after a 7 h 20 min incubation in high sucrose/glycogen ratio conditions: (a,b) negative staining; (c) cryo-TEM. Scale bars: 100 nm.

μm negative defocus of the objective lens), this suggests that the central part of the particles is more dense. The cryo-TEM image of one selected particle (Figure 4a) has been submitted to a low-pass circular Fourier filter in order to remove the high-frequency information (Figure 4b). This treatment enhanced the variation in amplitude contrast and confirmed the core−shell organization, the shell having a lower density than the core. By comparing cryo-TEM images of such particles with those

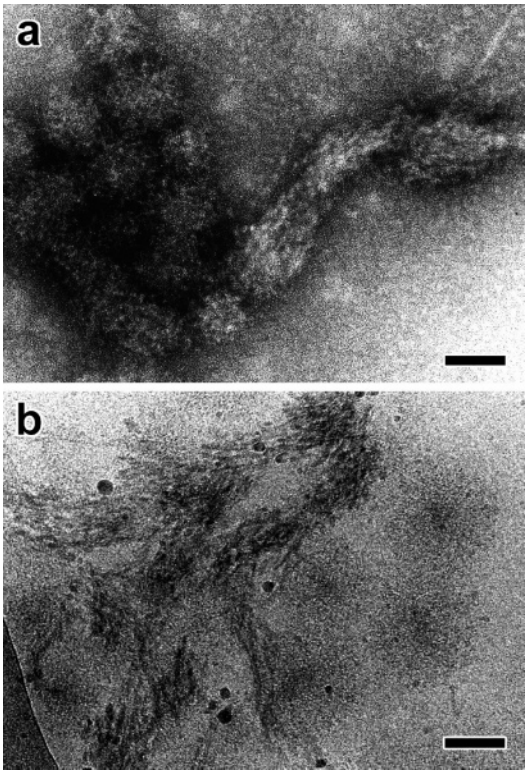

Figure 6. TEM images of the product obtained after a 13 h incubation in high sucrose/glycogen ratio conditions: (a) negative staining; (b) cryo-TEM. Scale bars: 100 nm.

of initial glycogen, we logically assumed that individual glycogen particles constituted the core of the objects.

Some of the objects observed after 7 h 20 min and 13 h incubations are very similar to those previously described. Particles of 100 nm diameter with a rugged surface are seen on negatively stained preparations (Figures 4a and 5a), whereas cryo-TEM images show 150 nm core−shell particles (Figures 4c and 5b). However, we also observed some fibrous material coexisting with the nanospheres (Figures 4b, 5a,b), its fraction being larger at 13 h than at earlier reaction times.

After an incubation of 23 h, aggregates that are a mixture of 100 nm particles and fibrous material are observed in TEM images of negatively stained preparations (Figure 6a−c). However, three types of objects can be identified in cryo-TEM images (Figure 6d−f): 150 nm core−shell particles similar to those observed at 2 h 45 min, 7 h 20 min, and 13 h, fibrous material and 100 nm particles that resemble those seen in the images of negatively stained preparations. Their contrast is also slightly stronger than that of the 150 nm particles, suggesting a higher density or crystallinity. As seen in Figure 6d,e, the fibrous material is made of connected ellipsoidal domains consisting of elementary elongated units with a width of 7−10 nm. The rather strong contrast with respect to the embedding ice may correspond to diffraction contrast and suggests that these units are semicrystalline.

Low Sucrose/Glycogen Ratio. After a 1 h incubation in LSGR conditions, aggregates of particles with an approximate diameter of 30 nm are observed. These particles are very similar to initial glycogen (Figure 7a,b). However, their overall shape is much less homogeneous, and small angular protrusions are seen on their surface. No isolated particle can be detected. Aggregates are also observed after an incubation of 4 h, the constituting particles being similar in size and aspect to those seen at 1 h

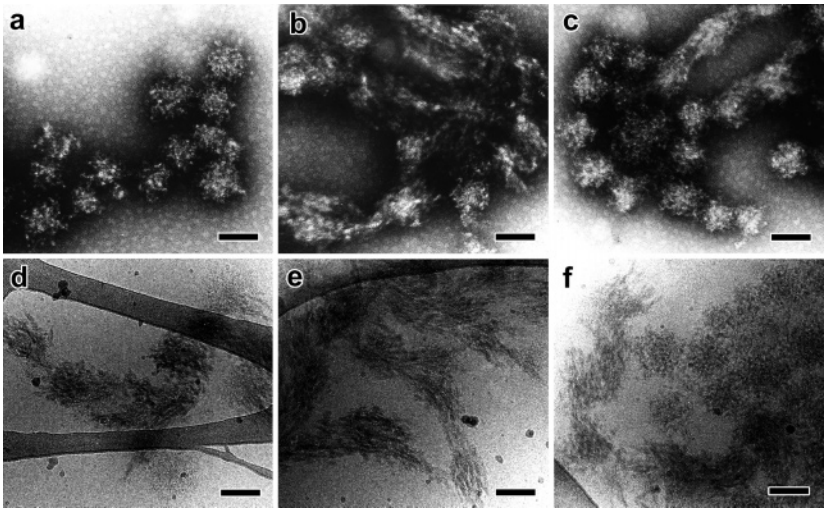

Figure 7. TEM images of the product obtained after a 23 h incubation in high sucrose/glycogen ratio conditions: (a−c) negative staining; (d−f) cryo-TEM. Scale bars: 100 nm.

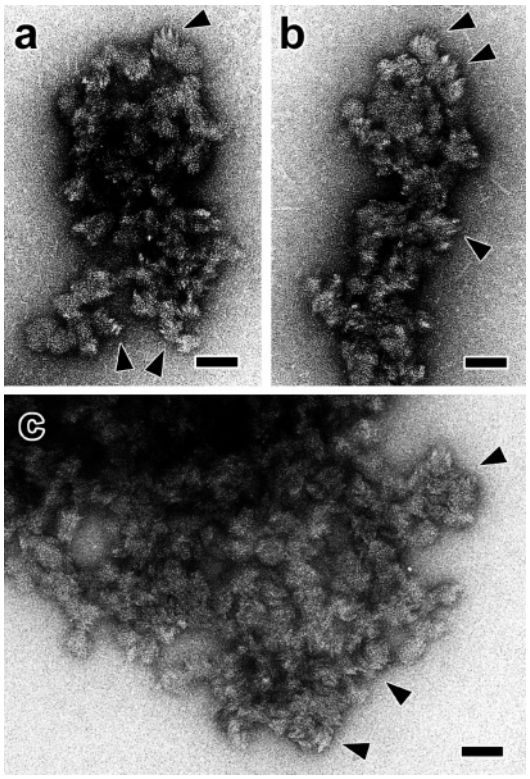

Figure 8. TEM images of the product obtained after 1 h (a,b) and 4 h (c) incubations in low sucrose/glycogen ratio conditions. Arrowheads indicate crystallites pointing out from the surface of the particles. Scale bars: 50 nm.

(Figure 8c). Cryo-TEM images of both samples (not shown) confirm the morphology observed on negatively stained specimens.

Crystallization. X-ray diffraction diagrams of the samples obtained in HSGR conditions at 2 h 45 min, 7 h 20 min, and 23 h are shown in Figure 9. The corresponding degrees of crystallinity are presented in Table 3. All recorded diagrams are characteristic of a pure B-type crystal structure, similar to that resulting from amylose or amylopectin recrystallization in water, with main diffraction peaks appearing at $2\theta = 5.7°$, 15°, 17°, 22°, and 24°. No crystallinity is detected at 1 h. Then, it increases up to 33% after 13 h and reaches a plateau thereafter. The increase observed after 7 h 20 min may correspond to the precipitation of the fibrous material observed in the TEM

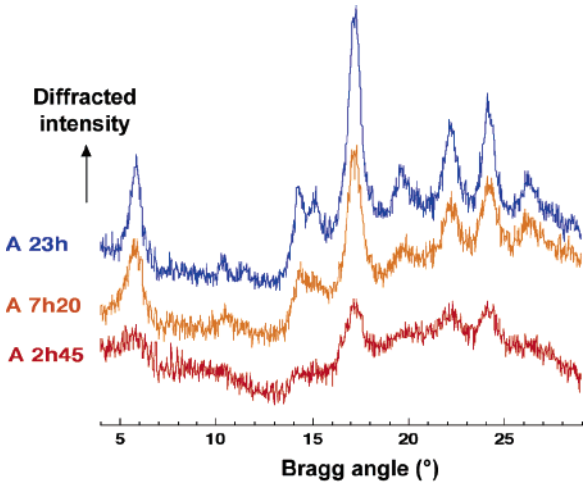

Figure 9. X-ray diffraction diagrams of glycogen after modification by amylosucrase in high sucrose/glycogen ratio conditions during 2 h 45 min, 7 h 20 min, and 23 h.

Table 3. Evolution of the Degree of Crystallinity and Lateral Crystal Size (from the (100) diffraction peak) with Incubation Time

time (h)	crystallinity (% ± 3%)	lateral crystal size (nm)
	High Sucrose/Glycogen Ratio	
1	0	nd
2.45	12	6.3
7.20	28	9.0
13	33	10.7
23	34	11.7
	Low Sucrose/Glycogen Ratio	
1	22	7.3
4	25	7.5

images, since no further modification of glycogen occurs during the enzyme action (Table 1). The lateral crystal size increases from 6.3 nm after 2 h 45 min up to about 12 nm at the final stage (Table 3). It shows that independent linear amylose chains can reorganize more easily in the fibrous material than the elongated external chains in modified glycogen particles. The same trend is found for the crystallite size extracted from the peak at $2\theta = 17°$. It is 7.8 and 11 nm at 2 h 45 min and 23 h, respectively (data not shown), but this peak contains several reflections, which makes the interpretation difficult.

For LSGR conditions, the crystallinity is 22% and 25% at 1 h and 4 h, respectively. It does not change significantly between 1 and 4 h. Therefore, the crystallization occurs very quickly, which is consistent with the total consumption of sucrose observed at 1 h. As no linear α-(1,4) chains are produced in these conditions, the crystallinity is only due to the crystallization of elongated chains at the surface of glycogen particles. The lateral crystal size never exceeds 7 nm. The X-ray diffraction diagrams recorded in these conditions contain a broad amorphous scattering band similar to that of pure glycogen. The X-ray scattering diagram of glycogen was subtracted with a scaling factor adjusted in order to have a null intensity on the baseline between the diffraction peaks (not shown). The adjustment leads to a value of 0.64 which corresponds to the part of the initial amount of glycogen (30 g/L) in the final product (46.8 g/L). It shows that almost all elongated chains are involved in the crystallized fraction formed around the glycogen particles.

Discussion

According to the data previously published,[27] the kinetics and the yield of the products synthesized by amylosucrase in the presence of both sucrose and glycogen are clearly controlled by the donor/acceptor ratio. Four reactions compete during sucrose consumption:

(1) glucosyl transfer onto water (sucrose hydrolysis), leading to glucose formation;

(2) successive glucosyl transfers onto the glucose molecules released by sucrose hydrolysis (α-(1,4) chain polymerization), yielding maltooligosaccharides and longer linear chains;

(3) glucosyl transfer on the fructose released in the medium (sucrose isomerization), yielding turanose and trehalulose formation;

(4) glucosyl transfers on the external glycogen chains (glycogen glucosylation), leading to chain elongation.

The preferential direction of the catalysis toward some of these reactions is governed by the affinity of amylosucrase for the various acceptors and their relative concentration in the reaction medium.

In the reaction carried out using HSGR conditions, the glycogen molecules are not sufficiently concentrated to compete efficiently with other acceptors (glucose, linear chains in elongation, and fructose). The yield of glycogen glucosylation is smaller than that of linear chain polymerization. However, the elongation of glycogen chains is sufficient to visualize a significant increase in particle diameter by TEM. The mechanism of glycogen extension is schematically summarized in Figure 10. In a first stage (Figure 10a), the surface chains of the initial glycogen particles (IGP) are elongated, forming a homogeneous corona of extended linear glucan chains (LGC). As no more glucose incorporation in glycogen is detected after 7 h 20 min, the chains reach a maximum length (Figure 10b), then entangle, forming a network of double helical segments that would further associate into crystallites (Figure 10c) and lead to a shrinkage of the corona. Entanglement and subsequent crystallization only occur between elongated chains that are attached to the same glycogen particle. No particle cross-linking was observed, probably due to the low concentration of glycogen which did not favor interparticle contacts. This partial crystallization may restrict the accessibility of the nonreducing ends of the external chains to amylosucrase active site. This suggested mechanism would explain why 150 nm particles are detected in cryo-TEM images of the products obtained at 2 h 45 min

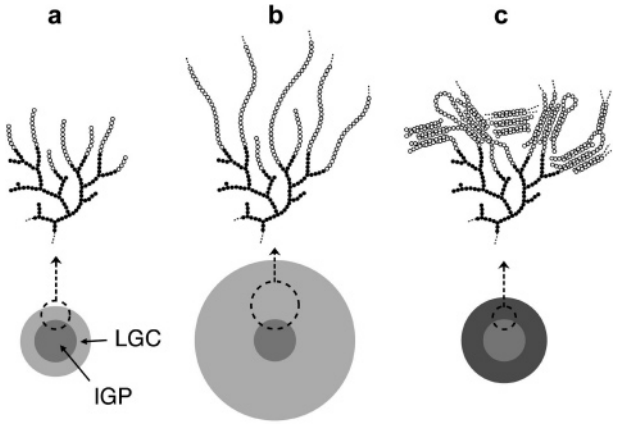

Figure 10. Scheme describing the possible growth mechanism and structural transformation of dendritic nanoparticles prepared in high sucrose/glycogen ratio conditions: (a) The surface chains of an initial glycogen particle (IGP) are extended by amylosucrase. ● and ○ correspond to the glucosyl units from glycogen and those incorporated by amylosucrase, respectively. (b) The chains are further elongated, forming a corona around the glycogen core. (c) The elongated chains form double helical segments by intra- and interchain entanglement. The double helices assemble to form crystallites, resulting in a shrinkage of the corona and an increase in density and crystallinity. For clarity, only short double helical segments have been drawn, and their connection with the glycogen particle has not been systematically indicated. The interaction of the external chains with the amylose-like polymer coproduced from sucrose has not been considered in the scheme.

(Figure 3b), 7 h 20 min (Figure 5c), and 13 h (Figure 6b), whereas 100 nm particles with a higher contrast, likely due to a higher density and semicrystallinity, are seen at 23 h (Figure 7f). The aspect of the 100 nm particles is rather similar to that of semicrystalline networks that are formed during amylose retrogradation.[34] The fact that 100 nm particles are seen at all stages in the images of negatively stained preparations (Figures 2a, 4a, 5a, and 6a) is probably due to the combined effects of staining and drying that result in a shrinkage of the corona.

The partial crystallization of the external chains of modified glycogen strongly decreases the affinity of the enzyme for the dendritic particles. Glucosyl units resulting from sucrose consumption are then preferentially transferred on glucose and maltooligosaccharides molecules, yielding linear amylose-like chains. Between 7 h 20 min and 23 h, all glucosyl units are used for the synthesis of amylose-like linear chains. The crystallinity and lateral crystal size increase markedly when the linear chains precipitate. The resulting semicrystalline fibrous material is sometimes associated to some elongated glycogen molecules. The crystallites present at the surface of the modified glycogen particles may act as nuclei for amylose precipitation and/or crystallization, as soon as appropriate concentration and chain length are reached. However, there is probably no covalent linkage between modified glycogen and amylose chains, since the fibrous material was well-separated by dissolution prior to chromatography. On electron micrographs, the fibrous material appears to be constituted of 7−10-nm-thick elementary units, which is consistent with the lateral crystal size measured by X-ray diffraction.

As is well-known for synthetic polymers,[35] such fibrillar growth may correspond to a preliminary stage in the formation of spherulitic and axialitic particles. The length of the α-(1,4) glucan coproduced in HSGR conditions is $\overline{DP}$ 35. This corresponds to the average length of the linear chains synthesized without glycogen from 600 mM sucrose alone, but differs from that of the amylose produced from 100 mM sucrose alone ($\overline{DP}$

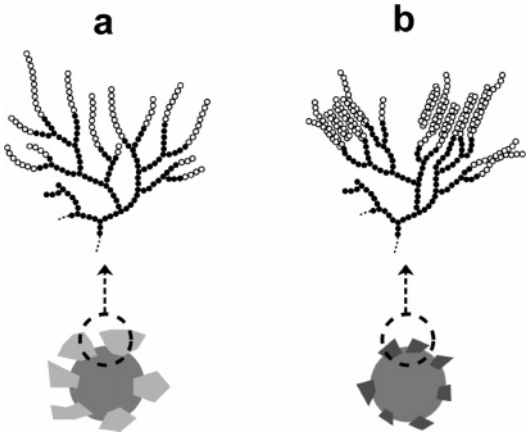

Figure 11. Scheme describing the structure of the glycogen particles after incubations carried out in low sucrose/glycogen ratio conditions: (a) The surface chains of a glycogen particle are heterogeneously extended by amylosucrase. ● and ○ correspond to the glucosyl units from initial glycogen and those incorporated by amylosucrase, respectively. (b) The elongated chains form double helical segments mostly by interchain reorganization. The double helices assemble to form crystallites resulting in an increase in crystallinity. For clarity, only short double helical segments have been drawn, and their connection with the glycogen particle has not been systematically indicated.

58).[25] Its morphology also completely differs, as fibrous material was observed in the present study, while networks, spherulites, and axialites were formed from sucrose alone.[25] This difference in both chain length and morphology is probably due to the simultaneous presence of the linear glucan and the modified glycogen in the synthesis medium. The relative solubility of linear α-(1,4) chains is thus reduced, and they precipitate with a lower chain length. This effect could be enhanced by induction of their precipitation at the partially crystallized surface of the modified glycogen particles. In LSGR conditions, glycogen particles are sufficiently concentrated to favor the elongation of the external chains of glycogen particles to the detriment of other reactions. With glycogen glucosylation being extremely rapid due to the strong affinity of amylosucrase for glycogen, all the initial sucrose is consumed after only 1 h. The resulting morphology is quite different. There is no significant increase in particle diameter by comparison to the initial glycogen, and small crystallites are seen heterogeneously distributed on their surface, but the overall shape of particles is more heterogeneous. With the number of external chains available for glucose transfer being 300 times higher than in HSGR conditions, the average elongation of each chain in glycogen is smaller for the same amount of transferable glucose molecules. Moreover, the high concentration of glycogen in the medium may modify the accessibility of some parts of the glycogen particles. Therefore, elongation of glycogen may be anisotropic. A possible mechanism for glycogen elongation in these conditions (LSGR) is schematized in Figure 11. In a first stage (Figure 11a), the surface chains of the initial glycogen particles are elongated, but to a lesser extent than in HSGR conditions. Then, as soon as chains are long and close enough, they intertwine into double helices which then associate into crystallites (Figure 11b). The crystallinity of the precipitate obtained after total sucrose consumption is 22%, which is remarkably high considering the small length of the elongated chains and the high relative amount of initial amorphous glycogen. The lateral crystal size is close to that obtained in HSGR conditions between 2 h 45 min and 7 h 20 min, which corresponds to the stage in the reaction that yields the highest incorporation of glucose into glycogen. The crystallization is very rapid, since crystallinity reaches a plateau at 1 h. This could be due to the high concentration of modified glycogen in the medium and the ability of short chains to crystallize quickly as soon as the precipitation starts.

As seen for amylose synthesized by amylosucrase from sucrose alone,[25] diluted longer chains slowly crystallize into networks, while more concentrated shorter chains suddenly precipitate and form aggregates of spherulitic or axialitic particles. With HSGR conditions, the increase in particle radius from 15 to 75 nm would correspond to an elongation of 60 nm. Assuming a pure double helical conformation which is the most extended conformation known for amylose and present in the B-type structures,[36] this would correspond to approximately 30 times the helical pitch and a degree of polymerization of 180. At 23 h, the aspect of the modified glycogen particles recalls that of networks formed by amylose precipitation in water. Unfortunately, as previously mentioned, it was impossible to determine by chromatography the length of the external chains of the modified glycogen after debranching by isoamylase. The only data we obtained is the $\overline{DP}$ of the α-(1,4) chains (of both the modified glycogen and the amylose-like polymer that is coproduced) at various reaction times, calculated from the λ_{max} values of their complexes with iodine. However, these values ($\overline{DP}$ 82, 127, and 113 at 2 h 45 min, 7 h 20 min, and 23 h, respectively) are underestimated due to the presence of a significant fraction of linear $\overline{DP}$ 35 α-(1,4)-glucan chains in the reaction media. The impact of the coproduction of the amylose-like polymer on the decrease of the λ_{max} value is significant between 7 h 20 min and 23 h, as the weight ratio between the modified glycogen and the amylose-like polymer decreased from 0.42 to 0.22.

On the contrary, with LSGR conditions, no significant increase in particle radius was observed. An increase of 5 nm would correspond to an elongation of 2−3 helical turns, i.e., about 15 monomers, which would explain why only small crystallites are seen on the particle surface. This value is in agreement with the length of the external branches of the modified glycogen determined by HPAEC−PAD after debranching with isoamylase. Indeed, the number of glucosyl units in the longer branches reaches 43, versus 31 for the longer chains in the initial glycogen. The $\overline{DP}$ of the modified glycogen calculated from the λ_{max} of its complex with iodine is 34. This value does not seem to be consistent with the HPAEC−PAD data recorded on the debranched modified glycogen, which shows the weight predominance of chains with DP 6−15. However, the discrepancy can be explained by the fact that linear chains with DP <20 do not complex iodine.[30] Finally, the extensive aggregation observed in the LSGR sample may be explained by the high concentration of modified particles in the medium and some partial entanglement of chain ends at the surface of crystallites that belong to neighboring particles.

This work highlights the potentiality of amylosucrase for the production of a new type of carbohydrate-based dendritic nanoparticle. Although they do not exhibit the highly symmetrical architecture of synthetic carbohydrate-based dendrimers,[37−39] sometimes called "sugar balls",[40] their preparation did not require any chemical reaction and was performed in aqueous medium using a rather simple procedure. Two natural substrates, namely, glycogen and sucrose, were used besides amylosucrase which catalyzed the elongation of glycogen external chains. The thickness and structure of the corona of these particles can be adjusted by controlling the initial sucrose/glycogen weight ratio and incubation time.

The particles formed using high sucrose/glycogen ratio conditions have a very specific core−shell structure. The maximum diameter of the particles was reached very rapidly, the growth being limited by two mechanisms: (i) the reorganization/recrystallization of extended linear chains on the surface of glycogen; (ii) the competitive elongation/crystallization of independent linear chains in solution. This work opens some interesting routes to tailor new types of α-D-glucans with specific properties. For instance, to prepare more or less slowly digestible carbohydrates, the resistance to α-amylases may be adjusted by controlling the length of the elongated chains and the structure resulting from their entanglement.

The core−shell structure of these particles may also be used to design nanocarriers with original properties. Indeed, linear α-D-glucan chains are known to form crystalline inclusion complexes in the presence of various molecules such as lipids[41] or aromatic compounds.[42] If such molecules were added to the HSGR incubation medium at a certain stage of chain extension, before the formation of double helical segments, single helical V-type crystallites may form, entrapping the complexing agents in the corona of the particles. One may then expect the release of the included compound during heating or enzymatic digestion. Of course, this mechanism is still speculative. Work is in progress to investigate the complexation properties of the dendritic particles.

Another promising aspect of our system is that it can be used to develop a biomimetic approach and reproduce in vitro the mechanisms involved in the biosynthesis of amylopectin and the structuring process of starch granules in plants. In a first paper, we reported on the structure of the glucans produced in a homogeneous system by an elongation enzyme from sucrose.[25] In the present work, the glucosylation by amylosucrase was carried out using glycogen particles as primers. The next step in this approach would be to introduce branching enzymes in the reaction medium and observe the structural changes that would result. The influence of a debranching activity may also be studied by adding isoamylase. It will then be interesting to investigate how the balance between each activity (elongation, branching, and debranching) in this simplified system will influence the growth and structuring of the dendritic glucan particles.

Acknowledgment. The authors are grateful to B. Pontoire and J. Davy (INRA Nantes, France) for the X-ray diffraction and differential scanning calorimetry measurements, respectively.

References and Notes

(1) French, D. In *Control of Glycogen Metabolism*; Whelan, W. J., Cameron, M. P., Eds.; Churchill: London, 1964; pp 7−28.
(2) Geddes, R. In *The Polysaccharides*; Aspinall, G. O., Ed.; Academic Press: New York, 1985; pp 283−336.
(3) Calder, P. C. *Int. J. Biochem.* **1991**, *23*, 1335−1352.
(4) Manners, D. J. *Carbohydr. Polym.* **1991**, *16*, 37−82.
(5) Yun, S.-H.; Matheson, N. K. *Carbohydr. Res.* **1993**, *243*, 307−321.
(6) Boyer, C. D.; Liu, K.-C. *Phytochemistry* **1983**, *22*, 2513−2515.
(7) Wong, K. S.; Kubo, A.; Jane, J.-L.; Harada, K.; Satoh, H.; Nakamura, Y. *J. Cereal Sci.* **2003**, *37*, 139−149.
(8) Mouille, G.; Maddelein, M.-L.; Libessart, N.; Talaga, P.; Decq, A.; Delrue, B.; Ball, S. G. *Plant Cell* **1996**, *8*, 1353−1366.
(9) Inouchi, N.; Glover, D. V.; Takaya, T.; Fuwa, H. *Starch/Staerke* **1983**, *35*, 371−376.
(10) James, M. G.; Robertson, D. S.; Meyers, A. M. *Plant Cell* **1995**, *7*, 417−429.
(11) Rani, M. R. S.; Shibanuma, K.; Hizukuri, S. *Carbohydr. Res.* **1992**, *227*, 183−194.
(12) Orrell, S. A.; Bueding, E.; Reissig, M. In *Control of Glycogen Metabolism*; Whelan, W. J., Cameron, M. P., Eds.; Churchill: London, 1964; pp 29−44.
(13) Matsui, M.; Kakut, M.; Misaki, A. *Carbohydr. Polym.* **1996**, *31* (4), 227−235.
(14) Boyer, C. D.; Damewood, P. A.; Simpson, E. K. *Starch/Staerke* **1981**, *33*, 125−130.
(15) Caldwell, R. A.; Matheson, N. K. *Carbohydr. Polym.* **2003**, *54*, 201−213.
(16) Melendez, R.; Melendez-Hevia, E.; Cnela, E. I. *Biophys. J.* **1999**, *77*, 1327−1332.
(17) Drochmans, P. *J. Ultrastruct. Res.* **1962**, *6*, 141−163.
(18) Drochmans, P.; Dantan, E. In *Control of Glycogen Metabolism*; Whelan, W. J., Cameron, M. P., Eds.; Churchill: London, 1968; pp. 187−201.
(19) Thomas, P.; Chambost, J.-P. *Biol. Cell.* **1978**, *33*, 235−242.
(20) Geddes, R.; Harvey, J. D.; Wills, P. R. *Biochem. J.* **1977**, *163*−*2*, 201−209.
(21) Harris, J. R. *Negative Staining and Cryoelectron Microscopy: The Thin Films Techniques*; Bios Scientific Publishers: Oxford, U. K., 1997.
(22) Putaux, J.-L.; Buleon, A.; Borsali, R.; Chanzy, H. *Int J. Biol. Macromol.* **1999**, *26*, 145−150.
(23) Potocki de Montalk, G.; Sarçabal, P.; Remaud-Siméon, M.; Willemot, R.-M.; Planchot, V.; Monsan, P. *FEBS Lett.* **2000**, *471*, 219−223.
(24) Albenne, C.; Skov, L.; Mirza, O.; Gajhede, M.; Feller, G.; d'Amico, S.; André, G.; Potocki-Veronese, G.; Van der Veen, B.; Monsan, P.; Remaud-Siméon, M. *J. Biol. Chem.* **2004**, *279*, 726−734.
(25) Potocki-Veronese, G.; Putaux, J.-L.; Dupeyre, D.; Albenne, C.; Remaud-Siméon, M.; Monsan, P.; Buléon, A. *Biomacromolecules* **2005**, *6* (2), 1000−1011.
(26) Rolland-Sabaté, A.; Colonna, P.; Potocki-Veronese, G.; Monsan, P.; Planchot, V. *J. Cereal Sci.* **2004**, *40*, 17−30.
(27) Potocki de Montalk, G.; Remaud-Siméon, M.; Willemot, R.-M.; Monsan, P. *FEMS Microbiol. Lett.* **2000**, *186*, 103−108.
(28) Potocki de Montalk, G.; Remaud-Siméon, M.; Willemot, R.-M.; Planchot, V.; Monsan, P. *J. Bacteriol.* **1999**, *181*, 375−381.
(29) Albenne, C.; Skov, L.; Tran, V.; Gajhede, M.; Monsan, P.; Remaud-Simeon, M.; André-Leroux, G. *Proteins*, in press.
(30) John, M.; Schmidt, J.; Kneifel, H. *Carbohydr. Res.* **1983**, *119*, 254−257.
(31) Wakelin, J. H.; Virgin, H. S.; Crystal, E. *J. Appl. Phys.* **1959**, *30*, 1654−1662.
(32) Klug, H.; Alexander, L. in *X-ray procedures*; Wiley-Interscience: New York, 1954; pp 491−538.
(33) Durrieu, V.; Putaux, J.-L.; Passas, R.; Gandini, A. *Microscopy and Analysis, European Edition* **2004**, *18* (1), 5−8.
(34) Putaux, J.-L.; Buleon, A.; Chanzy, H. *Macromolecules* **2000**, *33*, 6416−6422.
(35) Bodor, G. In *Structural Investigation of Polymers. Part II Polymer Morphology*; Ellis Horwood Series; in Polymer Science and Technology, Kemp, T. J., Kennedy, J. F., Eds.; New York, 1991; pp 144−177.
(36) Imberty, A.; Buleon, A.; Tran, V.; Perez, S. *Starch/Stärke* **1991**, *43*, 375−384.
(37) Jarayaman, N.; Nepogodiev, S. A.; Stoddart, J. F. *Chem.—Eur. J.* **1997**, *3* (8), 1193−1199.
(38) Turnbull, W. B.; Kalovidouris, S. A.; Stoddart, J. F. *Chem.—Eur. J.* **2002**, *8* (3), 2988−3000.
(39) Turnbull, W. B.; Stoddart, J. F. *Rev. Mol. Biotechnol.* **2002**, *90*, 231−255.
(40) Aoi, K.; Itoh, K.; Okada, M. *Macromolecules* **1995**, *28*, 5391−5393.
(41) Godet, M.-C.; Bizot, H.; Buléon, A. *Carbohydr. Polym.* **1995**, *27*, 47−52.
(42) Nuessli, J.; Putaux, J.-L.; Le Bail, P.; Buléon, A. *Int. J. Biol. Macromol.* **2003**, *33*, 227−234.

BM050988V